

Change in the effective dimensionality of multilayer V/Cu structures in a magnetic field

V. I. Dedi, V. V. Kabanov, A. G. Sandler, and A. S. Sidorenko

Institute of Applied Physics, Moldavian Academy of Sciences, Kishinev

(Submitted 6 August 1991; resubmitted 15 January 1993)

Zh. Eksp. Teor. Fiz. 103, 1662–1675 (May 1993)

A nonmonotonic temperature-dependent $3D \rightarrow 2D \rightarrow 3D$ dimensionality change has been observed in multilayer vanadium-copper structures in a parallel magnetic field. The observed changes in the temperature dependence of the critical fields $H_{c2}^{\parallel}(T)$ and of the critical exponents of the Aslamazov-Larkin fluctuation conductivity are explained by taking into account the temperature variation of two coherence lengths indicative of the proximity effect: the superconducting coherence length $\xi(T)$ and the normal metal coherence length $\xi_N(T)$.

1. INTRODUCTION

Size effects in layered anisotropic superconductors have been extensively studied in recent years. These studies have become particularly important after high- T_c superconductivity was discovered in layered metal-oxide compounds. The question of the dimensionality of high T_c superconductors is, apparently, one of the most important in elucidating the superconductivity mechanism in the latter. Artificially prepared superconducting layered structures (LS) are convenient model objects for the investigation of the size effects. In such structures superconducting layers alternate with layers of a dielectric (S/I structures), semiconductor (S/s structures), a normal metal (S/N structures), or another superconductor (S/S' structures). In S/I and S/s structures the interaction between S layers is determined by the Josephson tunneling across the structure, while in S/N and S/S' structures the interaction is provided by the proximity effect.

In artificial LS the dimensionality is determined by the ratio of the structure period Λ and superconducting coherence length $\xi(T)$. In the limit $\Lambda \ll \xi(T)$ the superconducting core embraces many layers so that a $3D$ state is realized. In the case $\Lambda \gg \xi(T)$ the core is localized in the S layer and a $2D$ state is observed. With further increase in Λ the $3D$ state may come back, if $d_s \gg \xi(T)$ (d_s is the superconducting layer thickness). The superconducting layers become effectively three-dimensional, i.e., the superconducting core does not interact with the S -layer boundaries.

Taking into account the temperature dependence of the coherence length, we can vary the LS dimensionality by varying not only the layer thickness, but also the temperature:

$$\xi(T) = \xi(0)(1 - T/T_c)^{-1/2}. \quad (1)$$

Near T_c we have $\xi(T) \gg \Lambda$, while far from T_c a $2D$ state can be realized for $d_s \sim \xi(0)$.

The crossover is quantitatively treated in Refs. 1–3 for structures with the Josephson interaction between the layers, and in Refs. 4–6 for S/N structures. To allow for the interlayer interaction, the transverse coherence length $\xi_{\perp}(T)$ characterizing the structure anisotropy is introduced in Ref. 1:

$$\xi_{\perp}(T) = \left[\frac{\Phi_0 H_{c2}^{\perp}}{2\pi(H_{c2}^{\parallel})^2} \right]^{1/2}. \quad (2)$$

The $2D \rightarrow 3D$ crossover occurs at a temperature T^+ , when $\xi_{\perp}(T^+) = \Lambda/\sqrt{2}$ where Λ is the structure period.

The dimensionality can be found from the quantitative analysis of the temperature dependences of the second critical magnetic field parallel to the layers. The temperature dependence $H_{c2}^{\parallel}(T)$ is given by the expressions^{7,8}

$$H_{c2}^{\parallel}(T) = \frac{\Phi_0}{2\pi\xi_{\perp}(T)\xi_{\parallel}(T)} \sim (T_c - T) \quad \text{for } 3D, \quad (3)$$

$$H_{c2}^{\parallel}(T) = \frac{\sqrt{12}\Phi_0}{\xi(T)d_s} \sim (T_c - T)^{1/2} \quad \text{for } 2D, \quad (4)$$

for the $3D$ and $2D$ states respectively, where $\Phi_0 = hc/2e$ is the magnetic-flux quantum and $\xi_{\parallel}(T) \equiv \xi(T)$ is the coherence length along the layers.

The crossover from the $3D$ anisotropic state to the $2D$ state was observed both in the LS with the Josephson interaction and in the structures with the proximity effect (see, e.g., Ref. 9). It was observed for the first time in the S/s structure Nb/Ge (65 Å/35 Å).¹⁰ The temperature dependences $H_{c2}^{\parallel}(T)$ of the critical magnetic field parallel to the layers showed a transition from a linear behavior near T_c to a square-root behavior as the temperature decreased. Similar results were next obtained for the S/s structures V/Si,¹¹ Pb/C,¹² and Pb/Ge,¹³ and also for the S/N and S/S' structures Nb/Cu,¹⁴ Nb/Ta,¹⁵ V/Fe,¹⁶ V/Ag,¹⁷ Nb/Nb_{0.6}Ti_{0.4},¹⁸ Nb/Ag,¹⁹ and Mo/V.²⁰ It is worth noting that the $3D \rightarrow 2D$ transitions are observed in the structures with intermediate interlayer coupling. For the structures with strong coupling the $H_{c2}^{\parallel}(T)$ dependence is linear in the whole temperature range ($3D$ state), while for the structures with weak coupling $H_{c2}^{\parallel}(T)$ obeys a square-root law ($2D$ state). This behavior was experimentally confirmed in Nb/Si (Ref. 21) and Nb_{0.52}Ti_{0.48}/Ge (Ref. 22; in these studies the thickness of the semiconductor layer was varied), and also in Nb/Cu (Ref. 13).

In addition to the $3D \rightarrow 2D$ crossover in the LS, a change in the dimensionality of superconducting fluctuations was reported in Ref. 23 where the fluctuation dia-

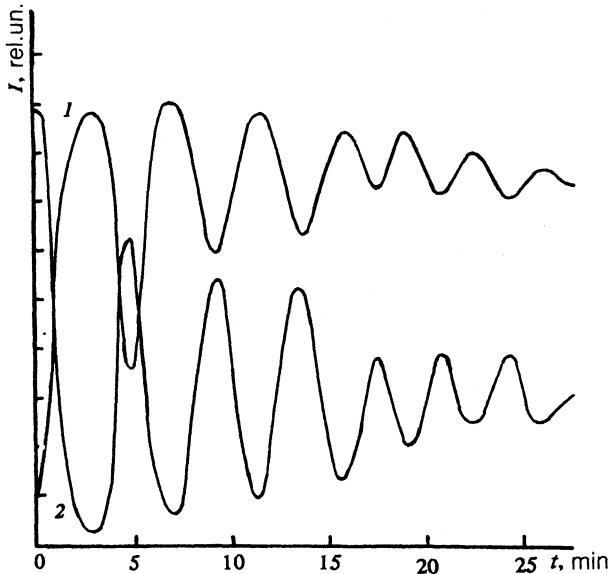


FIG. 1. Vanadium (1) and copper (2) line intensity versus etching time in the Auger analysis of the 100 Å/100 Å V/Cu sample.

magnetism of Nb/Si structures were studied, and also in Ref. 24 where the fluctuation conductivity of high- T_c $\text{YBa}_2\text{Cu}_3\text{O}_x$ monocrystals were investigated.

In the present study crossovers and superconducting fluctuations in layered V/Cu structures are investigated by measuring the critical magnetic field $H_{c2}(T)$ and the resistive $R(T)$ transition.

2. SAMPLE PREPARATION AND EXPERIMENTAL PROCEDURE

For the sample preparation we used the Z-400 high vacuum installation. The system was preliminarily evacuated by a turbomolecular pump down to 10^{-6} Torr. The samples were prepared by high frequency ion plasma evaporation. The evaporation was carried out in an argon atmosphere (99.99%) at a pressure $P_{\text{Ar}}=2 \cdot 10^{-3}$ Torr. Cathodes made of pure (99.99%) vanadium and a copper cathode made of a rolled Cu monocrystal were used to deposit the layers on substrates of monocrystal silicon with (100) orientation. When the layered structure was deposited, the substrate temperature was 150–200 °C. The evaporation rates were $v_V=3.7$ Å/s and $v_{\text{Cu}}=13$ Å/s.

The structures consisted of 10 vanadium layers of thickness $d_V=100\text{--}400$ Å and of 11 copper layers of thickness $d_{\text{Cu}}=100\text{--}200$ Å.

To monitor the quality of the prepared V/Cu samples we carried out mass spectrometric and Auger analyses with ion etching in depth. In Fig. 1 the results of the Auger analysis for a sample with $d_V=100$ Å and $d_{\text{Cu}}=100$ Å are plotted, namely, the intensity of vanadium (1) and copper (2) lines versus the etching time. The vanadium maxima clearly coincide with copper-concentration minima. It is worth noting that the Auger analysis does not give quantitative information on the LS interface, but it confirms qualitatively the periodicity of alternating vanadium and

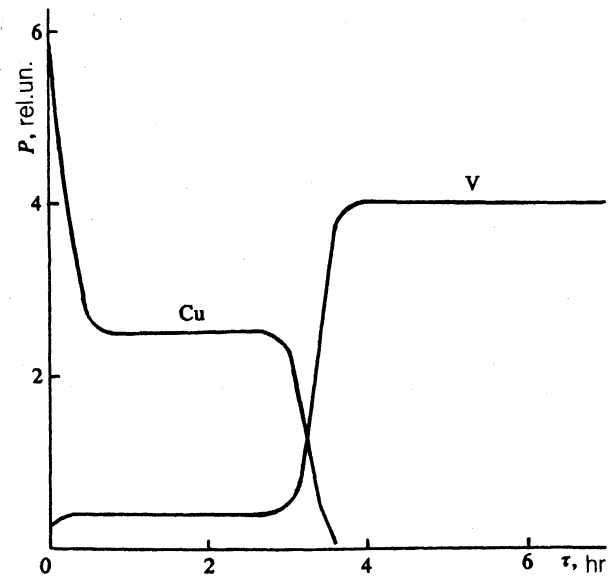


FIG. 2. V and Cu line intensity versus etching time in mass spectrometric analysis of the 250 Å/100 Å V/Cu sample.

copper layers. The results of the mass spectrometric analysis for two layers of the V/Cu structure ($d_V=250$ Å and $d_{\text{Cu}}=100$ Å) are shown in Fig. 2, with the etching time the abscissa and the flux of metal atoms in relative units the ordinate. The flux in the middle of V and Cu layers is taken as 100%. The analysis has shown that the transition region does not exceed 15 Å. There are 5–7% of vanadium atoms in a copper layer, and there is practically no copper (less than 1%) in a vanadium layer. The surface of the first Cu layer has a peculiarity which is accounted for by that in a near-surface layer copper is less strongly bonded and, for the same argon flux, more easily stripped.

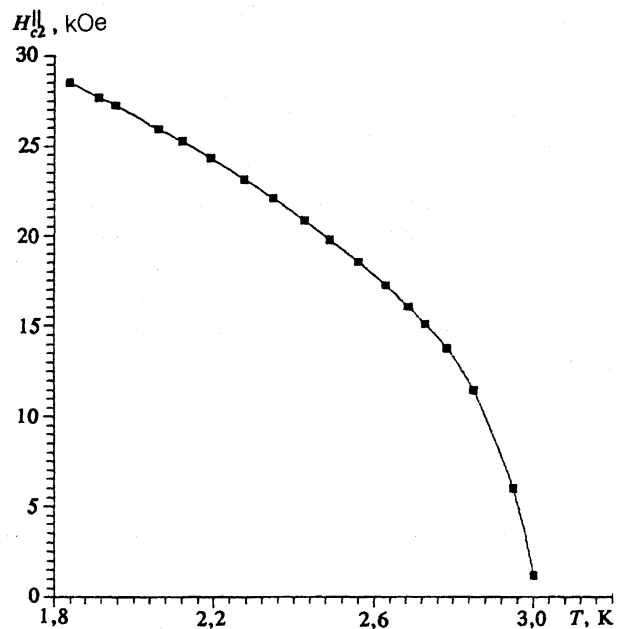


FIG. 3. The curve $H_{c2}^{\parallel}(T)$ for a single vanadium film of thickness $d=200$ Å.

TABLE I.

sample	d_V , Å	d_{Cu} , Å	T_c , K	$\rho_{300} \cdot 10^{-6}$, $\Omega \cdot \text{cm}$	$\gamma = \frac{\rho_{300}}{\rho_s}$	h^{\parallel} , kOe/K	h^{\perp} , kOe/K
1	250	100	4.69	15.59	2.60	7.1	4.5
2	250	150	4.55	23.21	3.01	7.0	5.5
3	250	200	4.43	28.17	3.10	10.0	—
4	200	150	4.32	16.11	2.52	8.5	4.5
5	200	100	4.11	14.16	2.13	6.5	3.5

The resistive transitions $R(H, T)$ were measured in an installation with a superconducting solenoid in which the magnetic field nonuniformity did not exceed $\pm 0.7\%$ over the length of 20 mm. A KG-100 cryostat had a system of helium vapor evacuation with a monostat providing temperature stability in the range 1.6–4.2 K to within 0.003 K. In the range 4.2–5 K temperature was stabilized by increasing and stabilizing the helium vapor pressure in the cryostat up to 2 bar. Temperature was measured with a GaAs thermometer which was outside the solenoid, and the magnetic field was monitored by a Hall generator positioned at the sample level. The sample was mounted on a special rod with a rotatable device allowing to vary the sample orientation in the magnetic field. To measure $R(H, T)$ we used the standard dc four-probe method.

3. RESISTIVE TRANSITIONS $R(H)$ AND TEMPERATURE DEPENDENCE OF THE SECOND CRITICAL MAGNETIC FIELD $H_{c2}(T)$ IN V/Cu STRUCTURES

To investigate the characteristics of separate superconducting layers comprising the superstructure, we prepared and studied single V films.

The parallel critical field of the studied vanadium layers (Fig. 3) in the whole temperature range obeys the law $H_{c2}^{\parallel}(T) \propto (1 - T/T_c)^{1/2}$, which should also be observed in the case of thin films meeting the condition $d \ll \xi(T)$.

For a layered V/Cu structure the temperature dependences of the second critical field are quite different from those in single vanadium films.

In Table I we list the parameters of V/Cu samples.

The values of the derivatives $h^{\parallel} = dH_{c2}^{\parallel}/dT$ and $h^{\perp} = dH_{c2}^{\perp}/dT$ have been calculated near T_c .

Figure 4 shows the function $R/R_{\text{res}}(H)$ in a parallel field for a V/Cu structure (250 Å/100 Å); R_{res} has been measured in strong magnetic fields suppressing superconductivity. Near $T_c(0)$ the transitions $R(H)$ are fairly narrow. As we move away from $T_c(0)$, the transitions become wider with increasing H_{c2} , while the structure undergoes a transition into the 2D state with separate two-dimensional superconducting layers. At low temperatures, however, the transitions $R(H)$ again become narrow. We can single out, at the end of the transition, a region of abnormally drastic decrease in resistance which gradually extends to the whole transition with decreasing temperature. For clarity, we have plotted in Fig. 5 the temperature dependences of the widths ΔH^{\perp} and ΔH^{\parallel} of superconducting transitions for the same sample. The behavior of ΔH for parallel and perpendicular field orientation is qualitatively different. In the case when the magnetic field is perpendicular to the layers and the superstructure does not affect the mixed state, ΔH^{\perp} grows in monotonically with decreasing temperature, whereas ΔH^{\parallel} changes in a complicated manner.

A similar behavior is found also for structures with other ratios of vanadium and copper layer thicknesses. It is important to note that as the thickness d_{Cu} of copper layers grows, the transitions $R(H)$ become narrower at lower temperatures. There are no anomalies on the $R(H)$ curves for perpendicular fields.

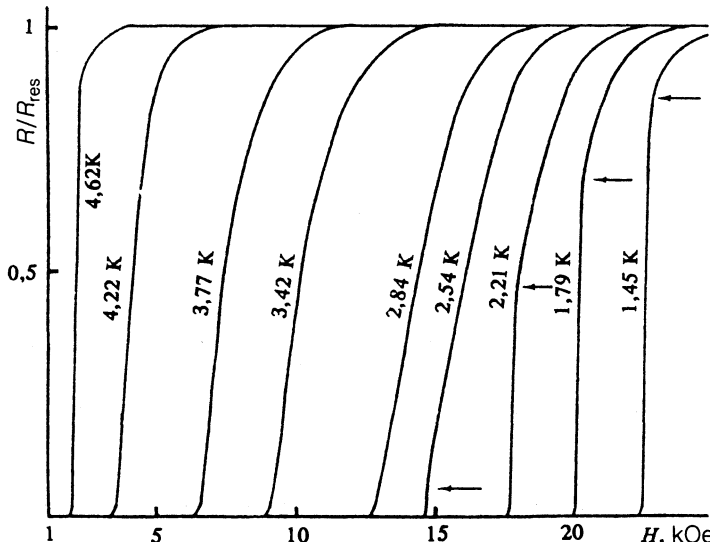


FIG. 4. The curve $R/R_{\text{res}}(H)$ in a parallel magnetic field for the 250 Å/100 Å V/Cu structure.

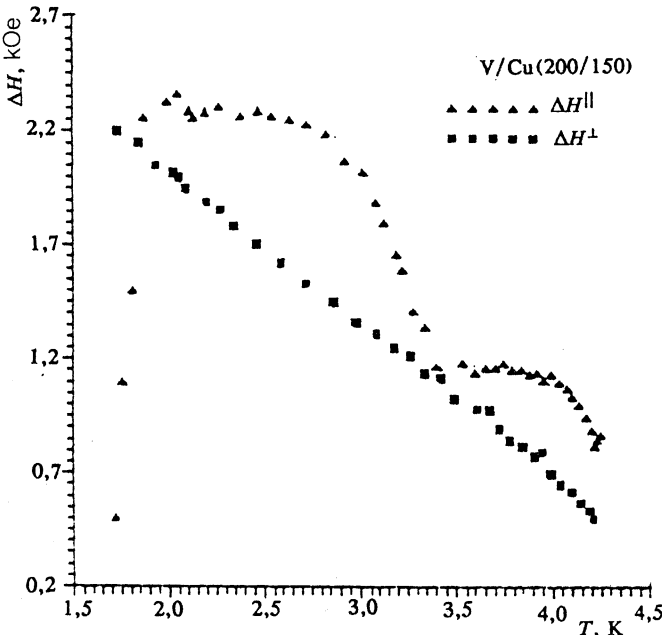


FIG. 5. The curves $\Delta H^\perp(T)$ and $\Delta H^{\parallel}(T)$ for the $250\text{ \AA}/100\text{ \AA}$ V/Cu structure.

The temperature dependences of the parallel and perpendicular magnetic fields, $H_{c2}^{\parallel}(T)$ and $H_{c2}^{\perp}(T)$, for the V/Cu structure with the thickness ratio $250\text{ \AA}/150\text{ \AA}$ are shown in Fig. 6. The value of H_{c2} is found for the level $0.5 \cdot R_{\text{res}}$ (the dependences do not change, if H_{c2} is found for other levels). The function $H_{c2}(T)$ shows a linear T dependence throughout the investigated temperature range, as is typical for layered structures.²³ Three regions can be singled out on the $H_{c2}^{\parallel}(T)$ curve. Near T_c the dependence is linear, $H_{c2}^{\parallel} \sim T_c - T$, and switches to a square-root one, $H_{c2}^{\parallel} \sim (T_c - T)^{1/2}$ away from T_c , in accord with the idea of a crossover ($3D \rightarrow 2D$) in this structure.¹⁵⁻²² At lower temperatures ($T \approx 0.4T_c$) a deviation from the square-root law is observed, and the temperature dependence $H_{c2}^{\parallel}(T)$ becomes linear again. This coincides in temperature with the change in the character of the $R(H)$ transitions and, evidently, has the same origin. The temperature T^* at which the square-root dependence (4) is replaced by the linear dependence (3) also decreases with the thickness d_{Cu} of the copper layers (see Table II).

The observed dependences of $R(H)$ and H_{c2}^{\parallel} can be accounted for if we assume that in the investigated temperature range a double crossover, $3D \rightarrow 2D \rightarrow 3D$, occurs in the system. This is considered at length in the next sections.

4. CHANGES IN THE EFFECTIVE DIMENSIONALITY OF FLUCTUATIONS IN THE V/Cu STRUCTURES

The observed change in the superconducting fluctuation dimensionality in the investigated V/Cu structures serves as further evidence in favor of the double ($3D \rightarrow 2D \rightarrow 3D$) crossover hypothesis.

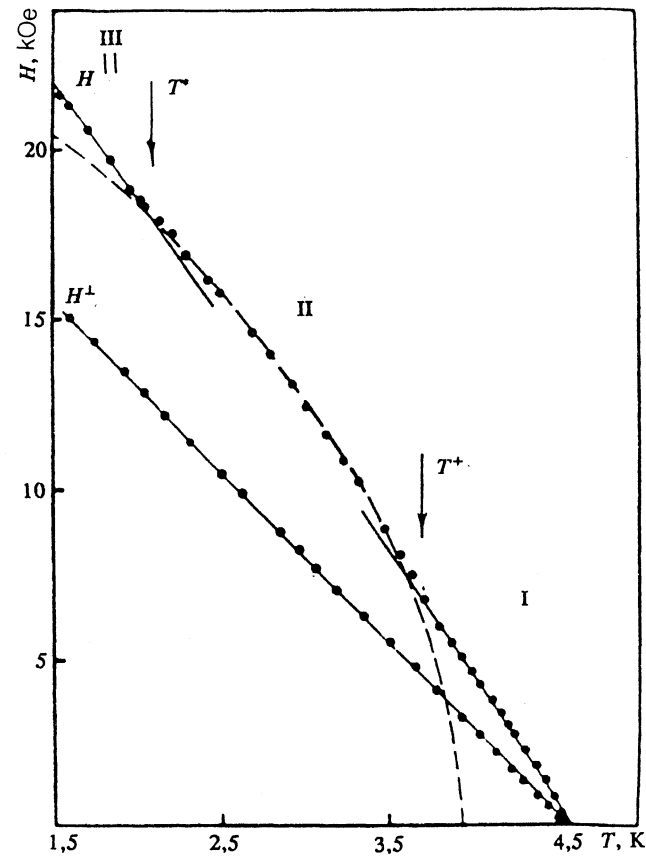


FIG. 6. The curves $H_{c2}^{\parallel}(T)$ and $H_{c2}^{\perp}(T)$ for the $250\text{ \AA}/150\text{ \AA}$ V/Cu structure.

The Aslamazov-Larkin (AL) fluctuation theory²⁵ describes the effect of fluctuation Cooper pairing on the sample conductivity σ at $T > T_c$, the fluctuation region ΔT_c and fluctuation conductivity σ' depending on the superconductor dimensionality:

$$\sigma' = \sigma - \sigma_n \sim (T/T_c - 1)^{D/2 - 2}, \quad (5)$$

where σ_n is the conductivity in the normal state, and D is the effective dimensionality ($D=1, 2$, and 3).

As noted above, in layered superconductors with strong anisotropy the dimensionality is temperature-dependent through the divergence of the superconducting coherence length $\xi_s(T)$ as $T \rightarrow T_c$. This divergence results in the growth of superconducting nuclei up to the dimensions exceeding the layered structure period, which is accompanied by the change in the fluctuation dimensionality at $T > T_c$ from $2D$ to $3D$. This effect was observed in high- T_c superconducting $\text{YBa}_2\text{Cu}_3\text{O}_x$ monocrystals,²⁴ when the fluctuation conductivity was studied.

The resistive transitions $R(T)$ of the V/Cu structure with $d_V = 250\text{ \AA}$ and $d_{\text{Cu}} = 100\text{ \AA}$ in different parallel magnetic fields are shown in Fig. 7. In zero field (curve 1) the transition is narrow, but becomes wider with increasing magnetic field (curve 2). In strong magnetic fields (curve 4) the transitions $R(T)$ are narrow again. Curve 3 corresponds to an intermediate transition from curve 2 to curve 4.

TABLE II.

sample	d_{V} , Å	d_{Cu} , Å	$\xi_{\perp}(T^+)$, Å	$\Lambda/\sqrt{2}$, Å	T^+ , K	T^* , K	H_{c2}^+ , kOe	H_{c2}^* , kOe
1	250	100	262	247	3.8	2.77	6.5	16.6
2	250	150	298	283	3.7	2.32	6.7	17.8
3	250	200	—	318	4.0	1.87	4.2	19.1
4	200	150	262	247	3.3	—	8.9	—
5	200	100	287	212	3.16	—	8.7	—

In Fig. 8 the measured fluctuation conductivity $\sigma'(T) = 1/R(T) - 1/R_n$ is compared with AL calculations (solid curves). It is found that in weak fields (curve a) the fluctuations are three-dimensional, in medium fields (curve b) they are two-dimensional and in strong fields (curve c) they are three-dimensional again.

Thus, temperature dependences of the fluctuation conductivity, $\sigma'(T)$, also exhibit the double $3D \rightarrow 2D \rightarrow 3D$ crossover. Probably, the nonmonotonic behavior of ΔH^{\parallel} (Fig. 5) is related to this crossover as well. In Ref. 26, where the transition broadening ΔH^{\parallel} of single vanadium films was studied, it was shown that when the fluctuation dimensionality decreases (from $2D$ in weak fields to $1D$ in strong parallel fields), ΔH^{\parallel} increases dramatically. In our case the $3D \rightarrow 2D$ crossover, decreasing the dimensionality results in the growth of ΔH^{\parallel} , while the second crossover ($2D \rightarrow 3D$), increasing the dimensionality, in the decrease in ΔH^{\parallel} .

5. ANALYSIS OF CAUSES OF DOUBLE CROSSOVER IN S/N STRUCTURES

The observed nonmonotonic behavior of the transition width $\Delta H^{\parallel}(T)$ and $H_{c2}^{\parallel}(T)$, and also of the fluctuation dimensionality in layered S/N structures is the consequence of the double $3D \rightarrow 2D \rightarrow 3D$ crossover in the investigated structures.

The first $3D \rightarrow 2D$ crossover which occurs near T_c has been thoroughly studied both theoretically and experimentally. As mentioned above, its cause is the decrease in the transverse coherence length $\xi_{\perp}(T) \sim (T_c - T)^{-1/2}$ with

decreasing temperature. When $\xi_{\perp}(T) \sim \Lambda$, the superconducting core is localized in the superconducting layer, and the system consists of weakly coupled $2D$ planes, whereas for $\xi \rightarrow \infty$ the core embraces a large number of S/N structure layers, and an anisotropic $3D$ case is realized. The temperature T^+ of the first crossover is determined by the condition

$$\xi_{\perp}(T^+) \approx \Lambda/\sqrt{2}$$

(see Ref. 14). In fact, this condition determines only the order of magnitude of $\xi_{\perp}(T^+)$, since in a real structure the S-N boundaries are always somewhat smeared. In Table II the values of $\Lambda/\sqrt{2}$ and $\xi_{\perp}(T^+)$ are listed for different structures. Taking into account everything mentioned above, a fairly good correlation of these quantities is observed. In the $250 \text{ \AA}/200 \text{ \AA}$ structure with a large value of Λ the $3D \rightarrow 2D$ crossover is shifted close to T_c and is not resolved.

The reverse crossover at low T can be related to one of two different mechanisms.

The first is connected with further decrease in the superconducting coherence length $\xi(T)$ with decreasing temperature. When the superconducting core decreases to $\xi_s(T) \ll d_{\text{V}}$, it becomes insensitive to the boundaries, and the vanadium layers become three-dimensional.

The second possible mechanism is connected with the growth of the coherence length $\xi_N(T) \sim (\hbar v_F l / 6\pi kT)^{1/2}$ in the normal metal as $T \rightarrow 0$, which leads to that the sample becomes isotropic and exhibits a three-dimensional behavior.

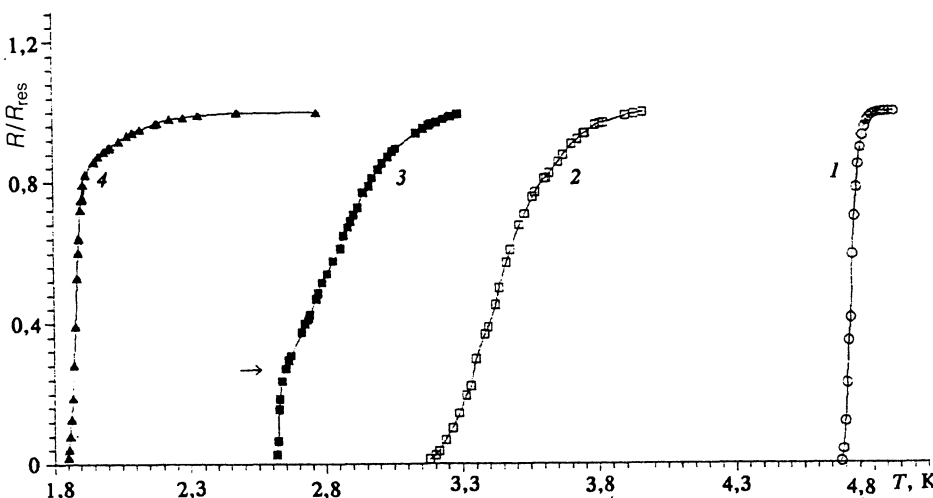


FIG. 7. The curves $R(T)$ in different parallel magnetic fields for the $250 \text{ \AA}/100 \text{ \AA}$ structure.

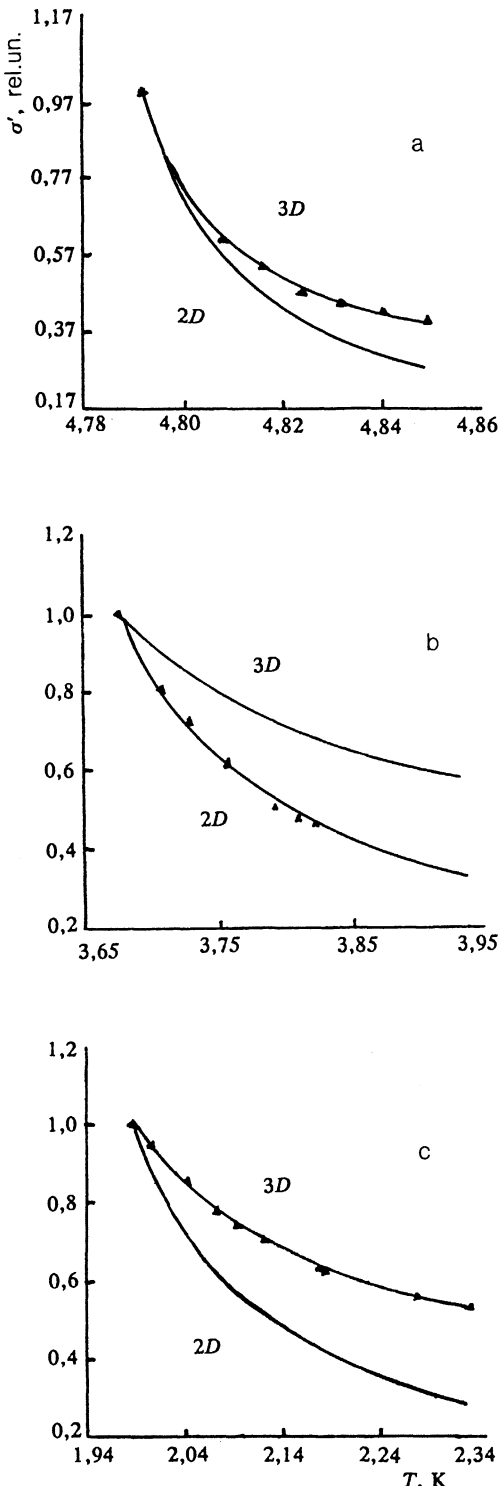


FIG. 8. The curves $\sigma'(T)$ for the 250 Å/100 Å structure.

The amplitude of the superconducting order parameter ψ_1 in normal layers, according to Ref. 27, is given by the expression

$$\psi_1 = 1 - \sqrt{2}d_N/\xi_N^2 - 2dx/\xi_N^2 + x^2/\xi_N^2, \quad (6)$$

where d_N is the normal layer thickness, and x is the coordinate normal to the layer. Though (6) is found for the contact of two superconductors with close critical temper-

atures, we believe that this expression can be used for qualitative analysis of our data. At low temperatures $\psi_1 \rightarrow 1$ due to the divergent $\xi_N \sim 1/\sqrt{T}$, which corresponds so that the V/Cu structure becomes isotropic and leads to a three-dimensional behavior $H_{c2}^{\parallel}(T) \sim (T_c - T)$.

To find evidence in favor of either mechanism, we studied the V/Cu structures with different V and Cu layer thickness and found for each structure the ratios T^*/T_c and $\xi(T^*)/d_V$, where T^* is the second crossover temperature.

The ratio T^*/T_c decreases with increasing copper layer thickness d_{Cu} :

$$\begin{aligned} d_{Cu} = 100 \text{ \AA}, \quad T^*/T_c = 0.59, \\ d_{Cu} = 150 \text{ \AA}, \quad T^*/T_c = 0.51, \\ d_{Cu} = 200 \text{ \AA}, \quad T^*/T_c = 0.40, \end{aligned}$$

which implies that for the second 2D–3D crossover to be realized, large values of ξ_N , i.e., lower temperatures, are needed.

On the other hand, the ratio $\xi(T^*)/d_V$ for the above samples (1–3 from Table II) is random

$$\begin{aligned} d_{Cu} = 100 \text{ \AA}, \quad \xi(T^*)/d_V = 0.71, \\ d_{Cu} = 150 \text{ \AA}, \quad \xi(T^*)/d_V = 0.32, \\ d_{Cu} = 200 \text{ \AA}, \quad \xi(T^*)/d_V = 0.51. \end{aligned}$$

Thus, the experimental data analysis for samples with different thicknesses d_{Cu} shows that the second mechanism of the 2D–3D crossover, when the V/Cu structures become isotropic due to the $\xi_N(T)$ divergence as $T \rightarrow 0$, is realized. It is important to note that in single thin films the dependences $R(H^{\parallel})$ and $H_{c2}^{\parallel}(T)$ similar to ours at $T > T_c$ are not observed.

Moreover, the dependence $H_{c2}^{\parallel}(T)$ for a single thin vanadium film (Fig. 2) indicates a purely two-dimensional behavior in the investigated temperature range. This also testifies to N layers being necessary for the reverse crossover observation.

6. CONCLUSION

The change in effective dimensionality—a double 3D–2D–3D crossover—found in layered V/Cu structures is described in terms of changes in dimensions of a superconducting core in a layered superconductor placed in a parallel magnetic field and of LS isotropization at low temperatures due to increasing coherence length in normal layers at $T \rightarrow 0$. Note that the second, 2D–3D, crossover observed on $H_{c2}^{\parallel}(T)$ curves is qualitatively similar to the Tachiki-Takahashi effect (observed in layered Nb/NbTi structures²⁸) but has a completely different origin. The TT effect connected with the switching of the core-formation field H_{c2}^{\parallel} from the clean superconductor (Nb) to the “dirty” one (NbTi) and accompanied by a break of the $H_{c2}^{\parallel}(T)$ curve is observed only in S/S' structures.

Additional evidence of the double, 3D–2D–3D, crossover in the studied LS is the change $\sigma'_{3D} \rightarrow \sigma'_{2D} \rightarrow \sigma'_{3D}$ in the fluctuation conductivity dimensionality in a parallel magnetic field.

The authors are grateful to N. Ya. Fogel' for useful discussions, and to P. A. Saltykov and T. Yu. Kuleshova for carrying out the Auger analysis.

- ¹R. A. Klemm, M. R. Beasley, and A. Luther, J. Low Temp. Phys. **16**, 607 (1974).
- ²N. Boccara, J. P. Carton, and G. Sarma, Phys. Lett. **49A**, 165 (1974).
- ³L. N. Bulaevskii, Zh. Eksp. Teor. Fiz. **65**, 1278 (1973) [JETP **38**, 634 (1974)].
- ⁴J. Simonin, Phys. Rev. B **33**, 1700 (1986).
- ⁵M. Tachiki and S. Takahashi, Physica **135B**, 178 (1985).
- ⁶M. Tachiki and S. Takahashi, Phys. Rev. B **33**, 4620 (1986).
- ⁷M. Tinkham, *Introduction to Superconductivity*, McGraw-Hill, 1975.
- ⁸W. E. Lawrence and S. Doniach, *Proceedings of the XII International Conference on Low Temperature Physics, Kyoto, Japan*, p. 361.
- ⁹B. Y. Jin and J. B. Ketterson, Adv. Phys. **38**, 189 (1989).
- ¹⁰S. T. Ruggiero, T. W. Barbee, and M. R. Beasley, Phys. Rev. Lett. **45**, 1299 (1980).
- ¹¹L. I. Glazman, I. M. Dmitrienko, V. L. Tovazhnyanskiy et al., Zh. Eksp. Teor. Fiz. **92**, 1299 (1987) [JETP **65**, 821 (1987)].
- ¹²J. P. Locquet, D. Neerink, and H. Van der Straaten, Jpn. J. Appl. Phys. **26**, 1431 (1987).
- ¹³J. P. Locquet et al., IEEE Trans. Magn. **23**, 1393 (1988).
- ¹⁴I. Banerjee and I. K. Schuller, J. Low Temp. Phys. **54**, 501 (1984).
- ¹⁵P. R. Brossard and T. H. Geballe, Phys. Rev. B **35**, 1664 (1987).
- ¹⁶H. K. Wong, B. Y. Jin, and H. O. Yang, Superlattices and Microstructures **1**, 2259 (1985).
- ¹⁷K. Kanoda, H. Mazaki, and T. Yamada et al., Phys. Rev. B **35**, 1664 (1987).
- ¹⁸M. G. Karkut, V. Matijasevic, and L. Antognaza, Physica C **153–155**, 473 (1988).
- ¹⁹M. Ikebe, Y. Obi, and Y. Kamiguchi, Jap. J. Appl. Phys. **26**, 1447 (1987).
- ²⁰A. J. Vermeer, C. W. Hagen, and D. G. de Groot, Physica C **162–164**, 409 (1989).
- ²¹C. Li, X. Cai, and Z. Ye et al., Layered Structures and Epitaxy. Materials Research Society Symposium Proceedings **56**, 177.
- ²²C. S. L. Chun, G. Zheng, J. L. Vincent, and I. K. Schuller et al., Phys. Rev. B **29**, 4915 (1984).
- ²³H. Obara, K. Uchinokura, and S. Tanaka, Physica C **157**, 37 (1989).
- ²⁴A. Kapitulinik, Physica C **153–155**, 520 (1988).
- ²⁵L. G. Aslamazov and A. I. Larkin, Fiz. Tverd. Tela **10**, 1104 (1968) [Sov. Phys. Solid State **10**, 875 (1968)].
- ²⁶A. S. Sidorenko, N. Y. Fogel, and V. G. Cherkasova, Physica B **108**, 993 (1981).
- ²⁷A. A. Abrikosov, *Fundamentals of the Theory of Metals*, North Holland 1988.
- ²⁸M. G. Karkut, V. Matijasevic, and L. Antognaza et al., Physica C **153–155**, 473 (1988).

Translated by E. Khmelnitski